Production cross sections of isotopes formed by fragmentation of ∼1*A* GeV ^{80}Kr beam

T. Yamaguchi,[1] T. Ohnishi,[2] T. Suzuki,[1] F. Becker,[3] M. Fukuda,[4] H. Geissel,[3] M. Hosoi,[1] R. Janik,[5] A. Kelić,[3] K. Kimura,[6] S. Mandel,[3] G. Münzenberg,[3] S. Nakajima,[1] T. Ohtsubo,[7] A. Ozawa,[8] A. Prochazka,[5] M. Shindo,[3,9] B. Sitár,[5] P. Strmeň,[5] T. Suda,[2] K. Sümmerer,[3] K. Sugawara,[1] I. Szarka,[5] M. Takechi,[4] A. Takisawa,[7] and K. Tanaka[2]

[1]*Department of Physics, Saitama University, Saitama 338-8570, Japan*
[2]*The Institute for Physical and Chemical Research (RIKEN), Saitama 351-0198, Japan*
[3]*Gesellschaft für Schwerionenforschung (GSI), D-64291, Darmstadt, Germany*
[4]*Department of Physics, Osaka University, Osaka 560-0043, Japan*
[5]*Faculty of Mathematics and Physics, Comenius University, 84215 Bratislava, Slovak Republic*
[6]*Nagasaki Institute of Applied Science, Nagasaki 851-0193, Japan*
[7]*Department of Physics, Niigata University, Niigata 950-2181, Japan*
[8]*Institute of Physics, University of Tsukuba, Ibaraki 305-8571, Japan*
[9]*Department of Physics, The University of Tokyo, Tokyo 113-0033, Japan*

(Received 21 August 2006; published 19 October 2006)

Production cross sections for the projectile fragmentation of a 1.05*A* GeV ^{80}Kr beam on a Be target were measured at the projectile fragment separator FRS at GSI. Cross sections were obtained for isotopes of the elements Ge to Kr close to the proton drip line. These data are compared to the results of the empirical parametrization EPAX and to abrasion-ablation calculations. We also compare the results to predictions of intranuclear-cascade calculations. The intranuclear-cascade calculations allow us to also compare well measured one-proton pickup cross sections.

DOI: 10.1103/PhysRevC.74.044608 PACS number(s): 25.70.Mn, 27.50.+e

I. INTRODUCTION

The proton drip line nuclei in the mass range $60 < A < 100$ are of particular interest because they determine the astrophysical rapid proton capture path [1,2]. To produce the nuclei to be studied in this region, low-energy fusion-evaporation reactions have been applied successfully for many years. Recently, high- and intermediate-energy projectile fragmentation has also proven to be a powerful tool for producing nuclei far from stability [3,4]. The SIS/FRS facility at GSI allows us to use projectile fragmentation at incident energies around 1*A* GeV to produce the nuclei of interest.

To assess the feasibility of radioactive beam experiments with these nuclei, it is important to know their production cross sections (σ_F). It is most desirable to predict the σ_F with physical models, such as the abrasion-ablation model [5]. Another approach is to use an empirical parametrization such as the EPAX formula [6,7]. The validity of both approaches must be checked by reliable experimental data.

For stable krypton projectiles, σ_F at intermediate energies have been measured with both proton- and neutron-rich projectiles. In contrast, σ_F at high energies have been obtained only with neutron-rich projectiles. Pfaff *et al.* measured σ_F from the reaction ^{78}Kr + ^{58}Ni at 75*A* MeV [8] and from the reaction ^{86}Kr + ^{27}Al at 70*A* MeV [9]. Data at high energies are only available for ^{84,86}Kr projectiles at 200 and 500*A* MeV, respectively [10,11].

The present study was performed to extend the current database by studying the fragmentation of the relatively neutron-deficient krypton isotope ^{80}Kr. In this article we present the systematics of σ_F measurements for neutron-deficient Kr to Ge isotopes.

II. EXPERIMENTAL PROCEDURE

The experiment was performed at the fragment separator facility FRS [12] of GSI at Darmstadt. A primary beam of ^{80}Kr accelerated by the SIS synchrotron to an energy of 1.05*A* GeV was directed onto a 1032 mg/cm^2 Be target at the entrance of the FRS. A typical intensity of 5×10^8 particles per spill was used to produce nuclei close to the drip line. Each spill lasted for approximately 800 ms and was extracted from the SIS every 2 s. Because σ_F were obtained during the course of a secondary reaction experiment [13], the fragments were identified in the first half of the FRS, with a selection only according to their mass-over-charge ratios. A total of three different settings of the FRS was used to select ^{72,74,76}Kr as the central fragments. For the ^{72}Kr setting, a 2512 mg/cm^2 thick Be target was used.

The experimental setup is sketched in Fig. 1. The secondary-electron transmission monitor SEETRAM [14] in front of the target was used to determine the primary beam intensity. At the first focus (F1), we placed a scintillation counter (thickness $t = 3$ mm) to obtain the start signal for a time-of-flight (TOF) measurement. This detector consisted of plastic scintillators (BC418) and photomultipliers (R2083 Hamamatsu PMT). PMTs were attached on both ends of the scintillator via straight shaped light guides [15]. This detector also served as an active slit for momentum definition ($\Delta p/p = \pm 0.2\%$). At the momentum-dispersive intermediate focus (F2) of the FRS (dispersion, 7 cm/%), we installed another scintillation counter (width $w = 120$ mm and $t = 3$ mm) and an ionization chamber (IC) [16] to obtain the TOF stop signal (flight path length $l = 17.8$ m) and to measure energy loss (ΔE), respectively.

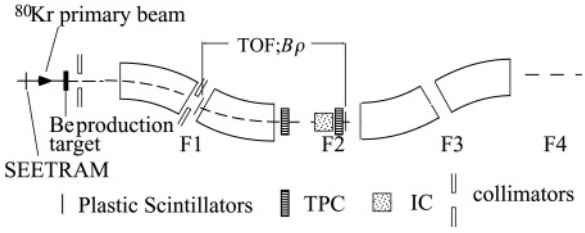

FIG. 1. Experimental setup at the fragment separator FRS

The TOF resolution of 33 ps Full Width at Half Maximum (FWHM) for the primary beam, as shown in Fig. 2(a), was sufficient to identify the particles unambiguously. The fragment nuclear charge number Z was determined by a ΔE measurement in an IC. It was calibrated with the primary beam for the nuclear charge $Z = 36$ [see Fig. 2(b)]. Position information at the foci F1 and F2 together with the magnetic field in the second dipole magnet gave the $B\rho$ of the fragments. This allowed us to calculate A/Z from the $B\rho$, TOF, and Z, providing particle identification. Note that the charge state q of the ions can be assumed at this beam energy to be identical to their nuclear charge numbers Z with a probability larger than 99.9%, according to the GLOBAL [17] calculations. Additionally, we positioned two time projection chambers (TPC) [18] at F2 to tune the separator and to monitor the emittance.

III. ANALYSIS AND RESULTS

A. Isotope identification

Figure 3(a) shows a typical particle-identification spectrum for the FRS setting that selects ^{72}Kr. Because we used a

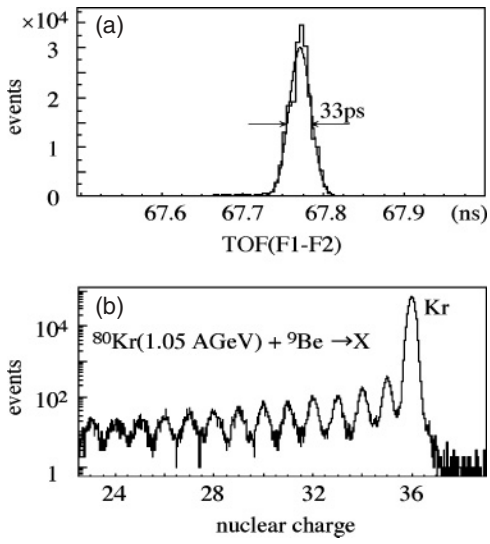

FIG. 2. (a) TOF spectrum between the scintillators at F1 and at F2. A Gaussian fit for the peak gives the time resolution of 33 ps (FWHM). (b) Nuclear charge spectrum of fragments from ^{80}Kr fragmentation at 1.05A GeV, measured in an ionization chamber. The primary beam with $Z = 36$ was used for calibration.

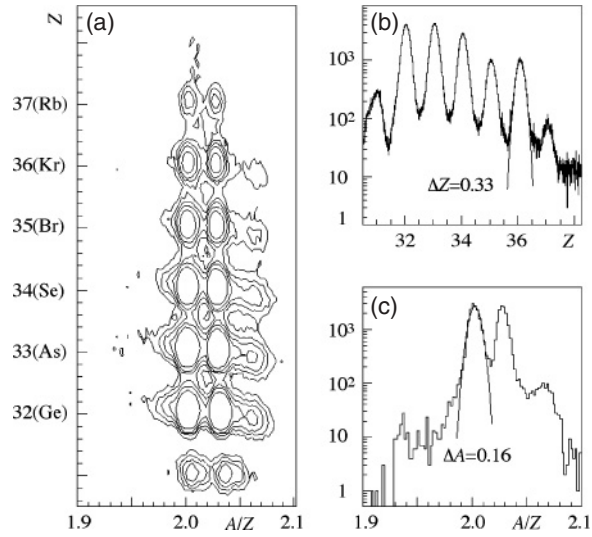

FIG. 3. (a) Two-dimensional contour plot of Z versus A/Z for the FRS setting selecting ^{72}Kr as the central fragment. (b) Z projection of Fig. 3(a). The solid line indicates a Gaussian fit to the $Z = 36$ peak, yielding a $\Delta Z = 0.33$. (c) A/Z projection spectrum for the $Z = 36.0 \pm 0.28$ slice of Fig. 3(a). The solid line indicates a Gaussian fit to the ^{72}Kr peak, yielding $\Delta A = 0.16$.

window discriminator on the scintillator pulse-height to reduce the trigger rate, the yield corresponding to $Z = 31$ isotopes was reduced. Thus only the isotopes ($\geqslant$32) are visible in the figure. We achieved good separation in both Z and A/Z, as shown in Figs. 3(b) and 3(c). In Fig. 3(b), a Z spectrum obtained by the projection of Fig. 3(a) is shown. A Gaussian fit for the $Z = 36$ peak gives a nuclear charge resolution of $\Delta Z = 0.33$ (FWHM). In Fig. 3(c), an A/Z spectrum obtained by the projection with a gate on $Z = 36.0 \pm 0.28$ is shown. A Gaussian fit to the ^{72}Kr peak gives $\Delta(A/Z) = 0.0042$, corresponding to a mass resolution of $\Delta A = 0.16$ (FWHM).

B. Determination of cross sections

Individual isotopic cross sections were calculated from the numbers of counts fulfilling a two-dimensional 2σ window condition in spectra where the nuclear charge Z is plotted versus the mass-to-charge ratio A/Z [See Fig. 3(a)]. The contamination was estimated to be less than 0.1%. Including the data acquisition the total identification efficiency for $Z > 31$ was determined to be 75%.

The transmission losses and losses due to secondary interactions were estimated by using the simulation code MOCADI [19]. The validity of MOCADI simulations was checked in our previous work, where we reported σ_F from ^{40}Ar fragmentation at $\sim$1A GeV [20]. For the central fragment of each tune of the FRS, the transmissions from target to F2 were calculated to be 8%–20%.

For the widths, σ, of the momentum distributions of the fragments, we used a modified Goldhaber formula (originally designed for *prefragments*, prior to evaporation) [21]: $\sigma^2 = \sigma_o^2 A_F(A_P - A_F)/(A_P - 1)$, where A_P and A_F refer to the projectile and fragment masses, respectively, and the width

TABLE I. Measured production cross sections (σ_F) for the fragmentation of a 1.05A GeV ^{80}Kr primary beam in a Be target.

Element	Z	A	σ_F (b)
Kr	36	76	$(6.1 \pm 1.8) \times 10^{-3}$
Kr	36	75	$(2.7 \pm 1.0) \times 10^{-3}$
Kr	36	74	$(1.7 \pm 0.5) \times 10^{-4}$
Kr	36	73	$(1.8 \pm 0.7) \times 10^{-5}$
Kr	36	72	$(5.3 \pm 1.8) \times 10^{-7}$
Br	35	74	$(8.8 \pm 2.6) \times 10^{-3}$
Br	35	73	$(3.5 \pm 1.4) \times 10^{-3}$
Br	35	72	$(2.7 \pm 0.8) \times 10^{-4}$
Br	35	71	$(4.2 \pm 1.7) \times 10^{-5}$
Br	35	70	$(9.2 \pm 2.6) \times 10^{-7}$
Se	34	72	$(1.6 \pm 0.5) \times 10^{-2}$
Se	34	71	$(4.2 \pm 1.6) \times 10^{-3}$
Se	34	70	$(7.0 \pm 2.2) \times 10^{-4}$
Se	34	69	$(1.2 \pm 0.5) \times 10^{-4}$
Se	34	68	$(2.7 \pm 0.8) \times 10^{-6}$
As	33	70	$(1.5 \pm 0.4) \times 10^{-2}$
As	33	69	$(3.3 \pm 1.3) \times 10^{-3}$
As	33	68	$(8.3 \pm 2.6) \times 10^{-4}$
As	33	67	$(1.1 \pm 0.4) \times 10^{-4}$
As	33	66	$(4.8 \pm 1.3) \times 10^{-6}$
Ge	32	68	$(2.1 \pm 0.6) \times 10^{-2}$
Ge	32	67	$(5.7 \pm 2.2) \times 10^{-3}$
Ge	32	66	$(1.1 \pm 0.3) \times 10^{-3}$
Ge	32	65	$(7.0 \pm 2.6) \times 10^{-5}$
Ge	32	64	$(4.8 \pm 1.8) \times 10^{-6}$

$\sigma_o = 90$ MeV/c is taken from experimental systematics. As an alternative method, we used the systematics of Morrissey [22] (designed for *postfragments*, after evaporation). The change in transmission was less than 10%, as expected for fragments relatively close in mass to projectile.

In Ref. [23] it was shown that for charge pickup processes the above momentum-width systematics lead to incorrect results. Therefore, the momentum widths for the charge pickup fragments ($Z = 37$) were estimated by using theoretical results from the code ISABEL+ABLA [5,23–25]. The transmissions from target to F2 were calculated to be around 2%.

The transmission-corrected numbers of counts for individual isotopes were converted to σ_F using the effective target thickness and the number of incident beam particles derived from the SEETRAM current digitizer. The σ_F values thus obtained are listed in Tables I and II.

TABLE II. Measured production cross sections (σ_F) for ($Z_{\rm proj} + 1$) fragments formed in the reaction ^{80}K (1050A MeV) + ^{9}Be.

Element	Z	A	σ_F (b)
Rb	37	78	$(7.4 \pm 2.2) \times 10^{-4}$
Rb	37	76	$(1.0 \pm 0.3) \times 10^{-4}$
Rb	37	74	$(4.5 \pm 1.6) \times 10^{-7}$

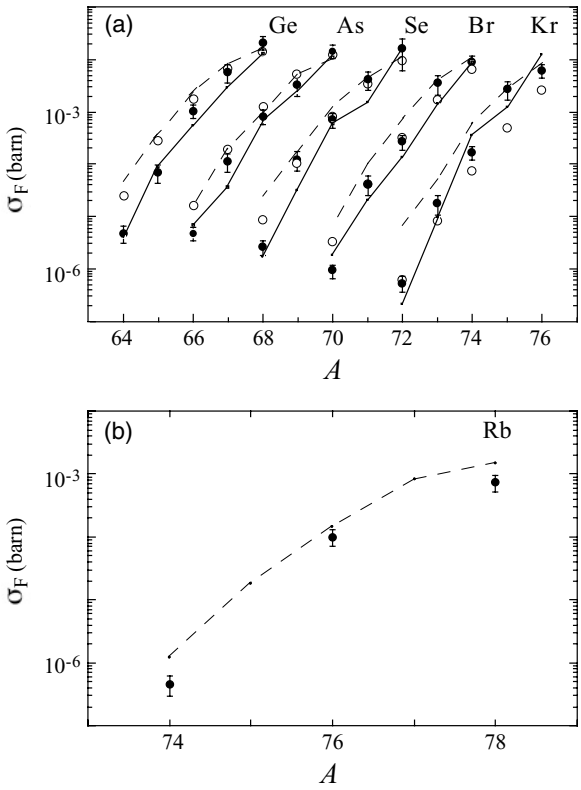

FIG. 4. (a) Production cross sections for the elements between krypton and germanium from the reaction ^{80}Kr + ^{9}Be at 1050 MeV/nucleon. The closed symbols indicate the measured σ_F. The open symbols represent the EPAX2 parametrization [7]. The solid lines stand for an abrasion-ablation (AA) model calculation. The dashed lines are predictions calculated with the intranuclear-cascade [24] plus ablation package ISABEL+ABLA [5,23,25]. (b) Production cross sections for ($Z_{\rm proj} + 1$) charge-exchange products ($_{37}$Rb isotopes). Filled circles denote the experimental data. The dashed line is a prediction calculated using ISABEL+ABLA.

IV. DISCUSSION

A. Cross sections of nucleon-removal products

The isotopic distributions for the elements Kr to Ge are shown in Fig. 4(a), together with the EPAX2 parametrization [7]. Considering that the range of cross sections determined in the present work extends over 5 orders of magnitude, EPAX2 predictions reproduce the tendency of the measured isotopic distributions relatively well. However, there are distinct discrepancies: the EPAX2 overpredicts the σ_F for nuclei close to the proton drip line except for the Kr isotopes. This overprediction toward the drip line has also been pointed out by Stolz *et al.* [26]. They reported the σ_F of $^{60-64}$Ge and of $^{64-68}$Se isotopes from the reaction ^{78}Kr + ^{9}Be at 140A MeV. The quasi-Gaussian shape that represents the neutron-deficient slope of the distributions in EPAX2 obviously needs some modification.

For a more physical understanding of the processes we compared the experimental cross sections with calculated ones from an intranuclear-cascade model (ISABEL, [24]) combined with an ablation code ABLA [5,23,25]). We ran about

5.5×10^5 intranuclear cascades, followed by 6 independent ablation sequences for each cascade. From the statistics obtained, we can predict cross sections down to a level of about 10 μb. The agreement between the experimental and the simulated data is good for the peripheral collisions at a cross-section level larger than 10^{-3} b, as shown in Fig. 4(a). They reproduce the tendency of the measured isotopic distributions relatively well. However, the calculations fail to reproduce the experimental data below 10^{-3} b. This might be because of the choice of parameters in the code, such as the excitation energy.

Second, we used a revised version of the geometrical abrasion-ablation model [5] as implemented in the LISE++ code [27]. This model assumes the nuclei to be spheres from which the geometrical overlap is abraded. The abrasion is followed by a simulated evaporation stage. We used the same parameters as those used in the literature [26]. For instance, an average excitation energy of 12 MeV per abraded nucleon is used, which is different from that used in code ABLA [5,23,25] of 27 MeV. Their calculation successfully reproduces the σ_F for the reaction ^{78}Kr + ^{9}Be at 140A MeV. The agreement between the experimental values and the predictions is better than the EPAX2 case as shown in Fig. 4(a).

B. Cross sections of charge pickup products

Nuclear charge-exchange reactions at relativistic energies are of interest because they allow one to draw some conclusions about the in-medium behavior of pions and deltas. Sümmerer *et al.* [28] measured isotopically resolved cross sections of $_{55}$Cs fragments from $^{129}_{54}$Xe + ^{27}Al and compared them to the intranuclear-cascade plus evaporation package (ISApace calculations) [28]. The measured Cs isotope distributions were well reproduced. In Ref. [23], (for the systems ^{209}Bi + $p, d,$ Ti) it could be shown, based on measured velocity distributions, that at relativistic energies quasi-elastic charge-exchange scattering and Δ-excitation both contribute to the formation of charge-exchange products. As a result, only masses equal to or lower than the projectile mass appear in the fragment distribution, and the cross sections are more than one order of magnitude smaller than those of neutron-removal products.

Similar results were observed for the formation of $_{37}$Rb charge pickup products in the present experiment. The calculated cross sections from ISABEL+ABLA [5,23–25] shown by the dashed line in Fig. 4(b) agree well with the measured ones. Though the present experiment cannot verify the model assumptions as detailed as Ref. [23], we conclude that the reaction mechanisms are well-described by an intranuclear-cascade plus evaporation model.

V. SUMMARY

We measured the production cross sections for fragments produced by ^{80}Kr fragmentation on a Be target at an incident energy of 1.05A GeV. These systematic measurements approached the drip line for Kr, Se, As, and Ge, and reached the proton drip line for Br, at a cross section level of 10^{-6} b.

The modified version of the empirical cross-section parametrization EPAX2 predicts the measured cross sections with good accuracy, but an overprediction toward the proton drip line in EPAX2 is observed. The intranuclear-cascade plus ablation ISABEL+ABLA calculation as well as the LISE++ calculations reproduce the measured cross sections with good accuracy.

We could also measure isotopically resolved cross sections for one-proton pickup that differ in magnitude by three orders. The intranuclear-cascade plus evaporation calculations reproduce the charge pickup cross sections.

ACKNOWLEDGMENTS

We thank the members of the FRS group and the SIS staff members for their help and K.-H. Behr, A. Bruenle, K. Burkard, and C. Karagiannis for their technical assistance. We thank Dr. J. Miller at LBNL for his careful reading of the manuscript. This work was supported in part by the Japanese Ministry of Education, Science, Sports and Culture by a Grant-In-Aid for Scientific Research under Program No. B(2) 16340063 and by VEGA, Slovakia.

[1] B. Blank, S. Andriamonje, S. Czajkowski, F. Davi, R. Del Moral, J. P. Dufour, A. Fleury, A. Musquère, M. S. Pravikoff, R. Grzywacz *et al.*, Phys. Rev. Lett. **74**, 4611 (1995).
[2] M. J. López Jiménez, B. Blank, M. Chartier, S. Czajkowski, P. Dessagne, G. de France, J. Giovinazzo, D. Karamanis, M. Lewitowicz, V. Maslov *et al.*, Phys. Rev. C **66**, 025803 (2002).
[3] C. Longour, J. Garcés Narro, B. Blank, M. Lewitowicz, Ch. Miehé, P. H. Regan, D. Applebe, L. Axelsson, A. M. Bruce, W. N. Catford *et al.*, Phys. Rev. Lett. **81**, 3337 (1998).
[4] T. Faestermann, R. Schneider, A. Stolz, K. Sümmerer, E. Wefers, J. Friese, H. Geissel, M. Hellström, P. Kienle, H.-J. Körner *et al.*, Eur. Phys. J. A **15**, 185 (2002).
[5] J. J. Gaimard and K.-H. Schmidt, Nucl. Phys. **A531**, 709 (1991).
[6] K. Sümmerer, W. Brüchle, D. J. Morrissey, M. Schädel, B. Szweryn, and Y. Weifan, Phys. Rev. C **42**, 2546 (1990).
[7] K. Sümmerer and B. Blank, Phys. Rev. C **61**, 034607 (2000).
[8] R. Pfaff, D. J. Morrissey, W. Benenson, M. Fauerbach, M. Hellström, C. F. Powell, B. M. Sherrill, M. Steiner, and J. A. Winger, Phys. Rev. C **53**, 1753 (1996).
[9] R. Pfaff, D. J. Morrissey, M. Fauerbach, M. Hellström, J. H. Kelley, R. A. Kryger, B. M. Sherrill, M. Steiner, J. S. Winfield, J. A. Winger *et al.*, Phys. Rev. C **51**, 1348 (1995).
[10] C. Stéphan, L. Tassan-Got, D. Bachelier, C. O. Bacri, R. Rimbot, B. Borderie, J. L. Boyard, F. Clapier, C. Donzaud, T. Hennino *et al.*, Phys. Lett. **B262**, 6 (1991).
[11] M. Weber, C. Donzaud, J. P. Dufour, H. Geissel, A. Grewe, D. Guillemaud-Mueller, H. Keller, M. Lewitowicz, A. Magel, A. C. Mueller *et al.*, Nucl. Phys. **A578**, 659 (1994).
[12] H. Geissel, P. Armbruster, K. H. Behr, A. Brünle, K. Burkard, M. Chen, H. Folger, B. Franczak, H. Keller, O. Klepper *et al.*, Nucl. Instrum. Methods B **70**, 286 (1992).
[13] T. Yamaguchi *et al.*, in preparation.

[14] C. Ziegler, Diploma thesis, Inst. für Kernphysik TU Darmstadt, 1992; A. Junghans, H.-G. Clerc, A. Grewe, M. de Jong, J. Müller, and K.-H. Schmidt, Nucl. Instrum. Method Phys. Res. A **370**, 312 (1996).
[15] S. Nishimura, M. Kurata-Nishimura, K. Morimoto, Y. Nishi, A. Ozawa, T. Yamaguchi, T. Ohnishi, T. Zheng, M. Chiba, and I. Tanihata, Nucl. Instrum. Methods A **510**, 377 (2003).
[16] A. Stolz, T. Faestermann, J. Friese, P. Kienle, H.-J. Körner, M. Münch, R. Schneider, E. Wefers, K. Zeitelhack, K. Sümmerer *et al*., Phys. Rev. C **65**, 064603 (2000).
[17] C. Scheidenberger, Th. Stöhlker, W. E. Meyerhof, H. Geissel, P. H. Mokler, and B. Blank, Nucl. Instrum. Methods B **142**, 441 (1998).
[18] V. Hlinka, M. Ivanov, R. Janik, B. Sitar, P. Strmen, I. Szarka, T. Baumann, H. Geissel, and W. Schwab, Nucl. Instrum. Methods A **419**, 503 (1998).
[19] N. Iwasa, H. Geissel, G. Münzenberg, C. Scheidenberger, Th. Schwab, and H. Wollnik, Nucl. Instrum. Methods B **126**, 284 (1997).
[20] A. Ozawa, O. Bochkarev, L. Chulkov, D. Cortina, H. Geissel, M. Hellström, M. Ivanov, R. Janik, K. Kimura, T. Kobayashi *et al*., Nucl. Phys. **A673**, 411 (2000).
[21] A. S. Goldhaber, Phys. Lett. **B53**, 306 (1974).
[22] D. J. Morrissey, Phys. Rev. C **39**, 460 (1989).
[23] A. Kelić, K.-H. Schmidt, T. Enqvist, A. Boudard, P. Armbruster, J. Benlliure, M. Bernas, S. Czajkowski, R. Legrain, S. Leray *et al*., Phys. Rev. C **70**, 064608 (2004).
[24] Y. Yariv and Z. Fraenkel, Phys. Rev. C **20**, 2227 (1979).
[25] A. R. Junghans, M. de Jong, H.-G. Clerc, A. V. Igatyuk, G. A. Kudyaev, and K.-H. Schmidt, Nucl. Phys. **A629**, 635 (1998).
[26] A. Stolz, T. Baumann, N. H. Frank, T. N. Ginter, G. W. Hitt, E. Kwan, M. Mocko, W. Peters, A. Schiller, C. S. Sumithrarachchi *et al*., Phys. Lett. **B627**, 32 (2005).
[27] O. B. Tarasov and D. Bazin, Nucl. Phys. **A746**, 411 (2004).
[28] K. Sümmerer, J. Reinhold, M. Fauerbach, J. Friese, H. Geissel, H.-J. Körner, G. Münzenberg, R. Schneider, and K. Zeitelhack, Phys. Rev. C **52**, 1106 (1995).